



Pathways of Water and Sediment in the Biesbosch Freshwater Tidal Wetland

Eveline C. van der Deijl¹  · Marcel van der Perk¹ · Hans Middelkoop¹

Received: 2 May 2018 / Accepted: 7 August 2018 / Published online: 11 September 2018
© The Author(s) 2018

Abstract

Diversion of water and sediment into drowning delta wetlands aims at renewed sediment accumulation for ecosystem regeneration and compensation of sea-level rise and soil subsidence. The success of such measures requires sound understanding of flow pathways and deposition patterns within wetlands and their feeding channels. This study aimed to (1) identify such pathways in a tidal freshwater wetland in the Netherlands, (2) determine the relative contribution of the two feeding rivers (Rhine and Meuse) to the water and sediment budget and (3) explore whether moving boat campaigns can contribute to a comprehensive understanding of the system. Bed level change was highest in newly developed areas, where equilibrium sets in. Sedimentation takes mainly place in channels close to the feeding rivers, where sediment becomes replenished each tidal cycle. Distal tidal channels receive only water poor in sediment during flood tide and experience erosion. Short term changes in suspended sediment load, measured during moving boat campaigns were generally consistent with average long-term changes in bed level. This means that short-term field measurements can not only be used to explain the processes, but also to predict the longer-term development of the major part of the study area.

Keywords Restoration · River deltas · Sediment budgets · Suspended sediment · Synoptic measurements · Tidal wetlands

Introduction

Although current flood protection measures, including dams, levees, storm-surge barriers, or other engineered structures, have been quite successful in reducing flood risk in deltas, the longer-term sustainability of such engineering measures have been called into question. The main reason for this is because they disrupt the morphodynamic processes and ecological functioning of the system, cannot cope with high end scenarios of Sea-Level Rise, and involve high costs for construction, maintenance and improvement (Hudson et al. 2008; Ibáñez et al. 2014; Temmerman and Kirwan 2015; Tessler et al. 2015). Therefore, alternative approaches have been put forward to re-establish the natural building of land, using the natural dynamics and resilience of the water system itself by restoration of the dynamic

hydrological, morphological and ecological processes of the river and delta wetlands (Brouwer and van Ek 2004; Hudson et al. 2008; Temmerman and Kirwan 2015).

Diverting water and sediment from major channels into adjoining areas to enhance sedimentation for land building is considered an effective strategy to prevent further wetland loss in case accretion due to production of organic material is limited. However, large differences in trapping efficiency and sediment budgets were not only found for different delta areas over the world, but also for different compartments within one delta. Mitsch et al. (2014), Lane et al. (2006), Noe et al. (2016), van der Deijl et al. (2017), and Verschelling et al. (2017) have shown that the supply of sediment is the major factor controlling the sediment budget and trapping efficiency of a compartment. This supply is not only controlled by the sediment load, but also by flow paths to the compartment (van der Deijl et al. 2017). Hence, to identify potential restoration areas and re-establish effective building of land in deltas with a rising sea, a thorough understanding of the system is essential (Temmerman and Kirwan 2015; Hua et al. 2016). For this, we need quantitative knowledge of flow paths of water and sediment, aggradation rates, and the mechanisms

✉ Eveline C. van der Deijl
e.c.vanderdeijl@gmail.com

¹ Department of Physical Geography, Faculty of Geosciences, Utrecht University, Utrecht, The Netherlands

controlling sedimentation and erosion in a delta system. Previous research has indicated the sedimentation rates and controlling factors of wetlands along rivers, estuaries, and coasts. However, very little attention has been paid to the hydro-morphodynamics of wetlands located in the transition zone between the fluvially dominated and tidally dominated zones of a river delta.

The research presented here provides one of the first field data-based assessments into the water flow and sediment dynamics in a freshwater tidal channel-wetland system, where new wetlands have been developed. For this, we aim to identify the flow paths of water and sediment in the Biesbosch, a small inland delta within the lower Rhine and Meuse delta, in the southwest of the Netherlands (see Fig. 1). This area forms a network of channels that connect previously embanked areas, in which water and sediment have been reintroduced by newly created river diversions. This channel-freshwater tidal wetland system serves to divert excess water during peak discharges of the Rivers Rhine and Meuse, but at the same time functions as dynamic ecosystem and trap of fluvial sediment. We take the advantage of differences in river connectivity and boundary conditions of the channels and their surrounding wetlands, which are however similar in climate conditions and tidal range. The differences in the boundary conditions are caused by the fact that the Biesbosch receives water and sediment from both the river Rhine and Meuse, of which the Meuse has a relatively low discharge and suspended sediment

concentration. Specific objectives of this study were to determine the major flow paths of water and sediment to, within, and out of the system and to determine the relative contribution of the feeding Rivers Rhine and Meuse to the sediment budget of the channels and surrounding wetlands. Moreover, this study explored the usefulness of synoptic moving boat measurements for gaining a quick overview of sediment transport and pathways in deltas within a short period of time. We hypothesize that synoptic moving boat measurements provide insight in the availability of sediment for land building within a short period of time. This is essential for the selection of river sections and adjacent potential restoration areas to re-establish effective building of land. Also, the effectiveness of newly created river diversions could be assessed in a short period of time after their implementation. For this purpose, we compared sediment budgets using existing series of observations of channel depth with sediment budgets derived from synoptic field surveys to document water flow and sediment concentrations within the Biesbosch freshwater tidal channel-wetland system.

Methods

Study Area

The Biesbosch comprises a 9000-ha freshwater tidal wetland in the lower Rhine and Meuse delta in the

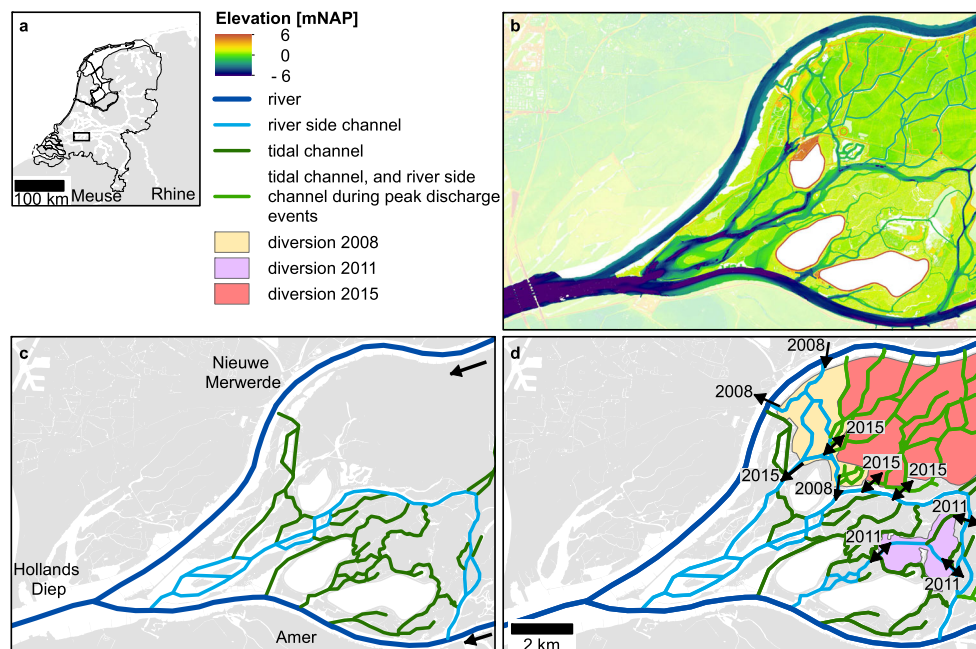


Fig. 1 Elevation above Dutch Ordnance Datum (m NAP) (**b**), schematisation of the main channels and their type before depoldering (**c**), and schematisation of the channels after depoldering (**d**) of the Brabantse

Biesbosch study area. The year of opening and the main flow direction of the new channels is given in (**d**)

Netherlands (see Fig. 1). The area developed after the catastrophic inundation of the area as a result of the St. Elisabeth flood, a combination of two North Sea storm surges and two floods of the River Rhine between 1421 and 1424 AD (Zonneveld 1959).

The Biesbosch has become a completely human-regulated area by local drainage and water level control of the polders, upstream weir management in the Rivers Rhine and Meuse, and the management of the downstream located Haringvliet storm-surge barrier. Because of this storm surge barrier, which has been operational since 1970, the tidal range in the study area has been reduced from approximately 1.9 m to 0.2 – 0.4 m (de Boois 1982). Consequently, the former areas with rush or reed culture developed to lush willow woods, grasslands, overgrown reed lands, and into embanked agricultural areas. Furthermore, the reduction of the tidal range has resulted in the development of shallow lagoons, the filling in of the deeper channels, a large decrease in intertidal area, and erosion of levees and banks. The channel banks are now often steep and - especially along the larger northeast-southwest oriented creeks - have been armoured by riprap to prevent erosion.

This research focused on the Brabantse Biesbosch, which is located between the River Nieuwe Merwede (in the north) and the River Amer (in the south), which are the downstream reaches of the respective Rivers Rhine and Meuse (Fig. 1). Water levels in the study area are influenced by the discharge of the Rivers Rhine and Meuse, tide, and wind direction and speed. Increased river discharge events are in general concurrent in the Rivers Rhine and Meuse. The tide is mixed semi-diurnal and has an average period of 12.5 hours, of which the tide rises on average 5 hours. Within the channel network, tidal amplitude increases with river discharge and with distance to the feeding river. Most creeks in this area are fed by the River Amer (Meuse), which enters the study area in the southeast and by the flood current from the southwest, which delivers also water of the River Nieuwe Merwede into the southwest of the study area. Although there is a tidal water level variation at the Nieuwe Merwede, there is no upstream flood current in this channel, not even during periods of low river discharge.

In the framework of the Room for the River (RfR) initiative, a large national flood prevention programme to improve the discharge capacity as well as the economic and environmental quality of the Dutch rivers (Rijkswaterstaat Ruimte voor de Rivier 2016), water and sediment have been diverted to previously embanked areas in the Biesbosch area. This action is also referred to as ‘depoldering’. Since 2008 water of the River Nieuwe Merwede also enters the northwestern part of the study area through a newly created inlet in the dike (see Fig. 1d). Other areas

have been depoldered in 2011 and 2015. Consequently, multiple channels have been changed from tidal channels (dark green in Fig. 1c) to second-order river channels (light blue in Fig. 1d). Furthermore, several channels (light green in Fig. 1d) have been developed during the depoldering in 2015. These channels are in general tidal dead-end channels, with a downstream connection to the old channel network. However, during high river discharges with elevated water levels, they become first order through-flowing side channels receiving water from the River Merwede via a spill-way at their upstream end.

Data Collection

To determine the sediment budget and the spatial pattern of sedimentation and erosion in the Brabantse Biesbosch freshwater tidal wetland, existing datasets as well as field measurements were used.

Bathymetric Data

The sediment budget and the spatial pattern of sedimentation and erosion in the existing navigable channels of the study area were determined using existing bathymetric data measured by Rijkswaterstaat. In 2007 and 2013, Rijkswaterstaat measured bed elevation of the channels using a multi-beam Simrad EM3002d echosounder combined with Netpos/long-range kinematic (LRK). The data were processed to a 1 m resolution grid in Quality Positioning Services (QPS) QUINSy 8.0 (Ad Schipperen (Rijkswaterstaat CIV), personal communication, 2015). The channel bed elevation in the area that was depoldered in 2008 (yellow in Fig. 1d) was measured in 2009 and 2012. The rate of change in bed level elevation was calculated by the difference in bed elevation divided by the time period passed between the bathymetric surveys.

Synoptic Sampling of Flow Dynamics

Within the period 26-11-2015 to 13-5-2016, 13 moving boat campaigns were carried out to obtain synoptic snapshots of water flow velocities, directions, and origin, and suspended sediment concentrations. During the moving boat campaigns turbidity, electrical conductivity, water depth, and flow velocities were measured. For this a Seapoint Turbidity Sensor, an Electrical Conductivity Sensor, a single beam echosounder, a GPS, and a Vertical Acoustic Doppler Profiler (VADCP) were mounted at the side of a steel boat at a depth of approximately 25 cm below the water surface. The steel of the boat interferes with the internal compass of the VADCP, so two additional aligned GPS systems were installed to determine the direction,

pitch and roll of the VADCP. The turbidity sensor was calibrated using water samples collected in the field. The suspended sediment concentration (SSC), water depth, and electrical conductivity (EC) were recorded each second. Flow velocities and channel discharge were determined by navigating a zigzag course with diagonal tracks across the channels.

Electrical conductivity measurements were used to distinguish the distribution and mixing of water from the River Rhine and River Amer, based on the higher electrical conductivity of Rhine water (Rijkswaterstaat 2018). The River Rhine has an average conductivity of 63.28 mS m^{-1} with a coefficient of variation of 0.11, while the electrical conductivity of the River Amer is on average 46.23 mS m^{-1} , with a coefficient of variation of 0.26. For each field campaign the electrical conductivity measurements were normalized with the electrical conductivity as measured in channel section Spijkerboor, which is completely filled with water from the River Amer.

Measurements took only place during daylight, so each campaign covered approximately 8 hours (two third) of the tidal period. Boat tracks and coverage of the tidal period are shown in Appendix, which shows the raw data of water flow relative to the tidal period, SSC and EC measured during the moving boat campaigns. The monitoring period was characterized by average discharges of the Rivers Rhine and Meuse, except for the field campaign on 17-02-2016, which took place during a slightly raised river discharge (see Fig. 2). Unfortunately, river discharges with a return period of more than 7 days per year did not occur during the monitoring period.

Data Analysis

Subdivision of the Study Area

To describe and compare the sediment budgets, established from existing series of observations of channel depth

with the sediment budgets derived from the synoptic field surveys, the channels of the study area have been divided in sections (Fig. 3). For this the study area was divided in four subareas, southeast, northeast, northwest, and southwest respectively. Tidal and river side channels were identified and numbered for these subareas. The river side channel section S7, had no upstream connection to the river before 2015 (Fig. 1d).

Channel Section Sediment Budgets

To determine the channel sections' sediment budget, cross-sections, perpendicular to the thalweg of the channel, were determined for each VADCP transect. For this the digital height model of the area and the main flow direction, as measured during the field campaigns was used. The suspended sediment load $SSL \text{ (g s}^{-1}\text{)}$ at a cross section was calculated using Eq. (1):

$$SSL = \sum_{i=1}^n SSC_i \times Q_i \quad (1)$$

Where n is the number of width increments in the cross section, SSC_i the mean suspended sediment concentration in the i^{th} increment of the cross section (g m^{-3}), and Q_i the discharge over the i^{th} increment, which is determined from the mean flow velocity over the increment (m s^{-1}), the mean water depth (m) and the increment width (m). For each cross section the flow weighted mean concentration (FWMC [g m^{-3}]) was determined to exclude the effect of differences in load, which may result from variations in the proportion of total channel width that was covered by the measurements. The FWMC was calculated with Eq. (2):

$$FWMC = \frac{SSL}{\sum_{i=1}^n Q_i} \quad (2)$$

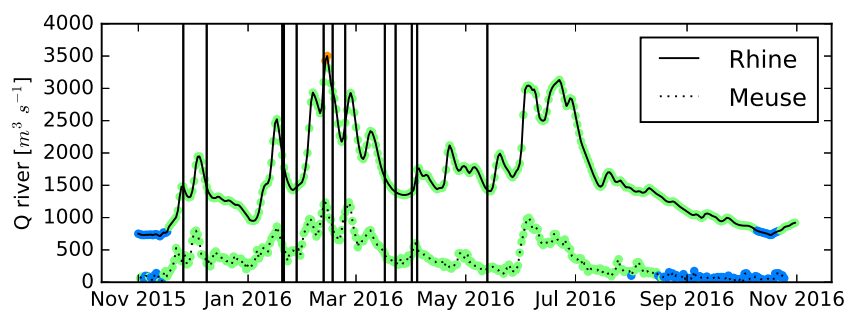


Fig. 2 The field campaigns are shown relative to the discharge of the River Rhine (Rijkswaterstaat measurement location Tiel, 48 km upstream (Rijkswaterstaat, 2018)), and River Meuse (Rijkswaterstaat measurement location Keizersveer, 1 km upstream (Rijkswaterstaat,

2018)). The colour shows the Rijkswaterstaat river discharge warning code, for lowered (blue, ± 13 days a year), normal (green, ± 343 days a year), raised (yellow, ± 7 days a year), high (orange, once in 5 to 10 years), or extreme (red, once in 1250 years) river discharge

In this equation, the total suspended sediment load (SSL [g s^{-1}]), is divided by the sum of the discharge over the increments (Q_i [$\text{m}^3 \text{s}^{-1}$]). The difference in suspended sediment Load (ΔSSL [g s^{-1}]) and the sediment trapping efficiency (E_{trap} [-]) between the upstream and downstream ends of the channel sections, was calculated using Eqs. (3) and (4):

$$\Delta SSL = (FWMC_{downstream} - FWMC_{upstream}) \times Q_{section} \quad (3)$$

$$E_{trap} = \frac{(FWMC_{downstream} - FWMC_{upstream}) \times Q_{section}}{FWMC_{upstream} \times Q_{section}} \quad (4)$$

Where $Q_{section}$ represents the average discharge over the channel sections ($\text{m}^3 \text{s}^{-1}$), and $FWMC_{upstream}$ and $FWMC_{downstream}$ the FWMC (g m^{-3}) at the start and end of the channel sections. The trapping efficiency of a channel section (see Fig. 3) was however only determined when the difference between the discharge at the up and downstream edge of the channel section is no larger than 20% of the upstream discharge.

The differences in SSL were standardized to gradients in SSL along a channel section, by dividing ΔSSL by the length of the sections, so channel section budget is shown per m channel length in $\text{g s}^{-1} \text{m}^{-1}$.

Results

Changes in Channel Bed Elevation

Figure 4 shows the change in channel bed elevation in m y^{-1} , between 2007 and 2013. For the northern part of the area, which was depoldered in 2008, the annual change in channel bed elevation was determined for the period 2009 - 2012. The figure shows that erosion takes place in the smaller tidal channels in the southwest of the study area, and near the inlet and outlet of the newly depoldered area. Sedimentation is observed in the wider and deeper channels. Locally, sedimentation takes place in the inner bend, while the outer bend erodes. Although e.g. the displacement of bedforms and outer bank erosion function as internal sources of sediment, the main source of sediment is external. Channel bed sedimentation was on average 12.8 mm y^{-1} during the period 2007 - 2013. Largest changes in bed elevation were observed in the newly de-poldered wetland (channel section S5), with maximum local bed level aggradation rates of about 1.0 m y^{-1} and local bed-level lowering rates of about 1.4 m y^{-1} .

Figure 5 presents the average change in channel bed elevation for the channel sections. Most channel sections show a rise of the channel bed level over the period 2007-2013, indicative for net sediment trapping. Especially, the northern part of the study area and all river side channels sections are characterised by a positive sediment budget. Negative sediment budgets are only found in tidal channel

Fig. 3 Tidal and river side channels for the southeast (T1-T9, S1-S3), northeast (T10-T13, S4), northwest (T14, S5-S7), and southwest (T15-T21, S8-S9) of the study area

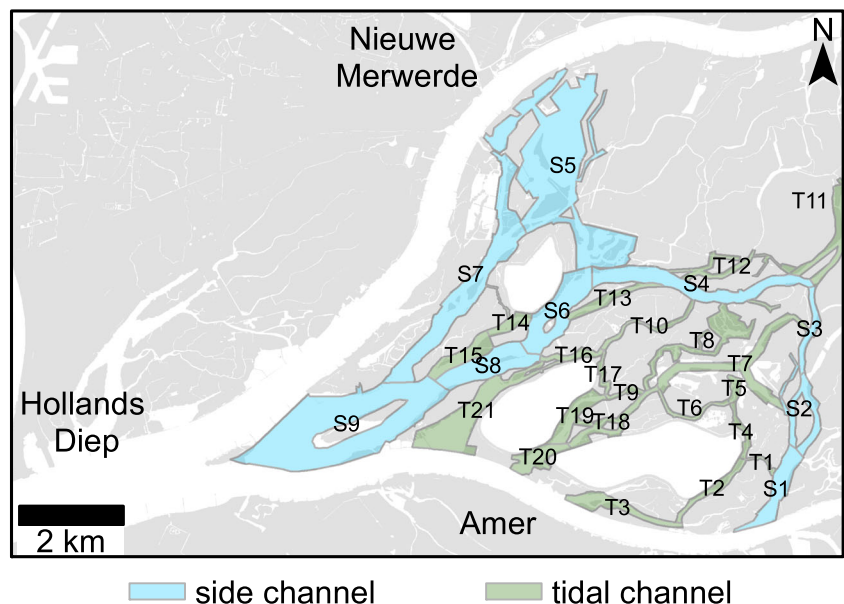
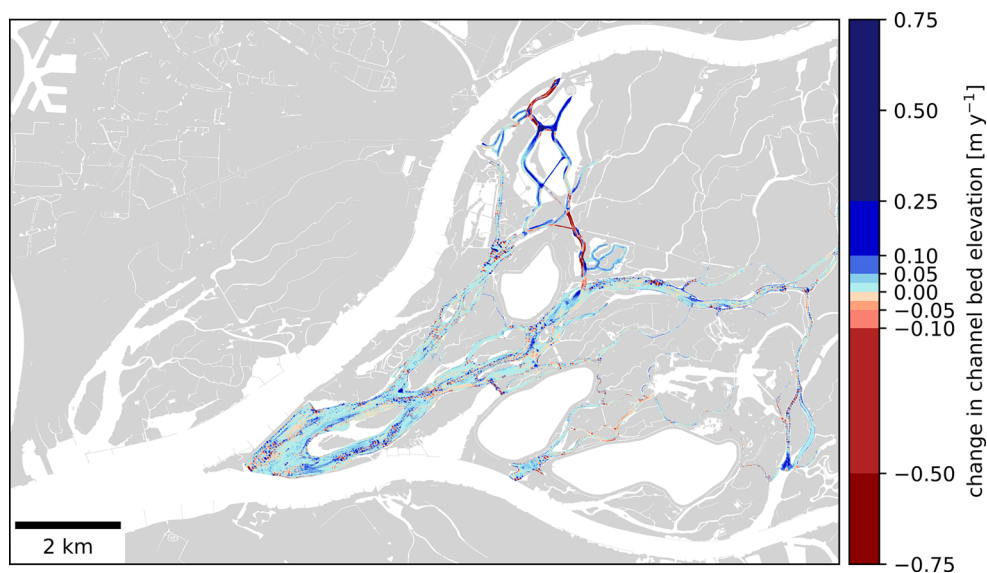


Fig. 4 The change in channel bed elevation in m y^{-1} over the period 2007–2013, and over the period 2009–2012 for the area, depoldered in 2008



sections T1, T4, T9, T17, and T18 in the southwest of the study area.

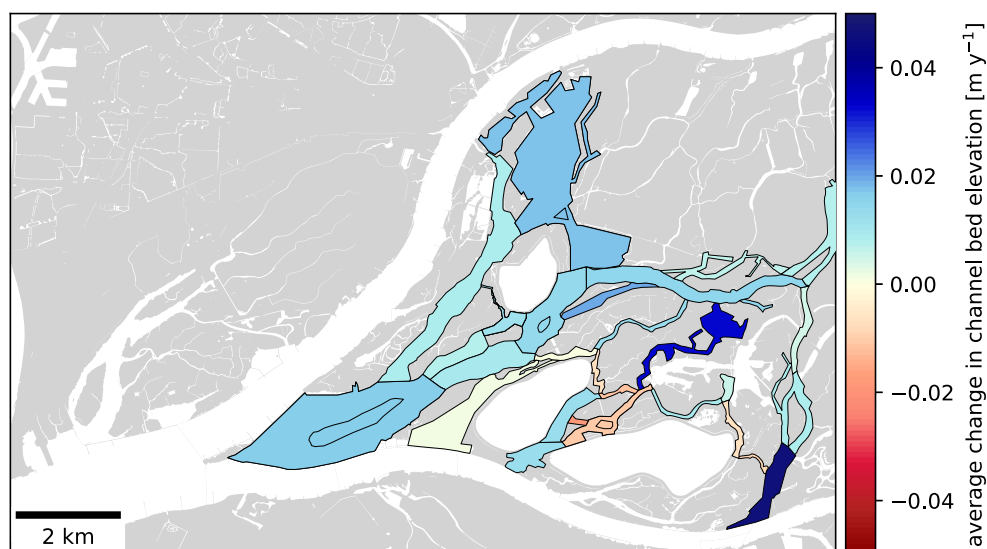
Flow Dynamics, SSC and EC

Measurement Data

Figure 6 shows the raw data of water flow, SSC and EC measured during the moving boat campaign of 01-04-2016 to illustrate the type of data and spatial patterns obtained during all field campaigns. This moving boat campaign occurred in clockwise direction through the study area,

starting during low tide in the southeast, with arrival at the start of flood tide in the southwest, high tide in the north and it ended during ebb tide in the southeast of the area. Figure 6 a shows the cross-sectional averaged flow velocity and direction. This figure also indicates that measurements in the study area were collected during different moments in the tidal cycle. Figure 6b and c show the lateral and longitudinal variation in suspended sediment concentration and electrical conductivity, as measured along the zigzag course. The satellite image in Fig. 6d shows an instantaneous snapshot of the spatial pattern of SSC at 1 April 2016 10:50AM. The location of the boat, at this

Fig. 5 Change in channel bed elevation [m y^{-1}] averaged over the channel sections.



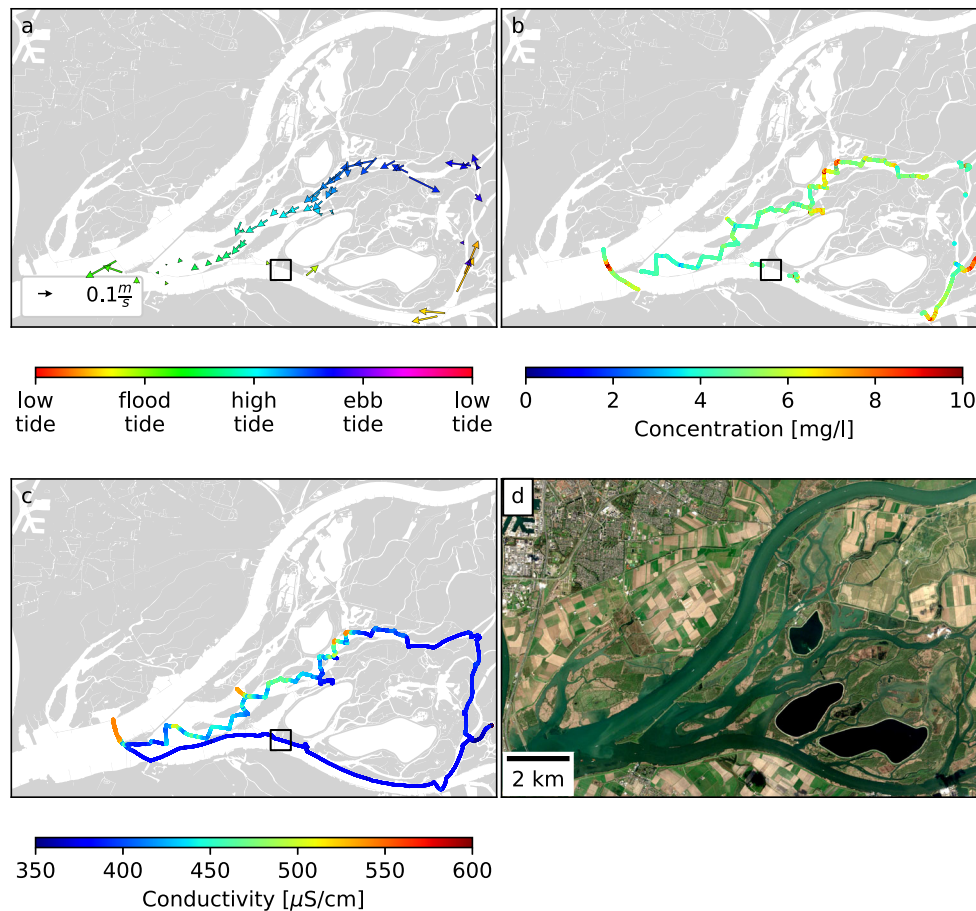


Fig. 6 Flow magnitude and direction during a tidal period (a), suspended sediment concentration (b), and electrical conductivity (c) of the moving boat campaign of 01-04-2016. The Sentinel2A RGB 10m

resolution image (d) was taken at 10:50. The location of the boat, at this moment, is indicated by the square in a, b and c

moment, is indicated by the square in Fig. 6a, b, and d. The raw data of the other field campaigns is shown in Appendix.

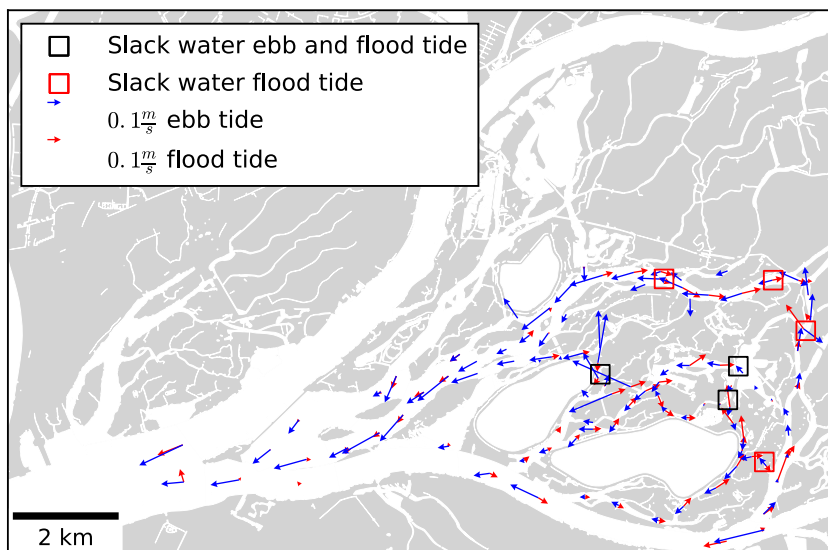
Flow Pathways

Figure 7 shows the distribution of the depth mean flow velocity of all monitoring campaigns, averaged over flood tide (red) and ebb tide (blue). The figure indicates most channels have a southwest orientation with flow to the southwest during ebb tide, and to the northeast during flood tide. The flow direction also changes in the smaller often north-south orientated tidal channels. However, no change in flow direction was observed in the larger north-south orientated side channel of the River Amer (channel section S1-S3), located in the east of the study area. In the tidal channels, the observed average and maximum flow velocities are larger for ebb ($0.12 - 0.48 \text{ m s}^{-1}$) than for flood tide ($0.09 - 0.17 \text{ m s}^{-1}$). Although a similar pattern

is observed in the river side channels, the magnitude of the flow velocities is slightly larger with values of $0.18 - 0.39 \text{ m s}^{-1}$ for ebb tide, and 0.10 up to 0.27 m s^{-1} during flood tide.

During flood tide of the individual measurement campaigns, slack water (red boxes in Fig. 7) was observed at different locations in section S4 in the northeast of the study area. The location of slack tide was observed more westwards for the monitoring campaigns with a relatively higher discharge of the River Amer. During the monitoring campaigns, slack water was observed both during flood and during ebb tide in channel sections T5, T7, and T17 (black boxes in Fig. 7). Since the secondly de-poldered area (purple in Fig. 1, tidal channel section T7 in Fig. 3) was developed to divert excess water of the River Amer during peak discharge events, it is likely that these zones of slack tide in channel sections T5, T7, and T17 of the study area move westwards or even disappear during peak discharge events of the River Amer.

Fig. 7 The depth mean flow velocity of all monitoring campaigns, averaged over flood tide (red) and ebb tide (blue). The square boxes show the locations of slack tide, as observed during the individual monitoring campaigns



The EC of the channel water is shown in Fig. 8, which shows the electrical conductivity relative to the measurements over across section S1 of the side channel of the River Amer (black box), for all field campaigns. The spatial variation in relative EC within the area reveals the relative contribution of Merwede and Amer water within the channel network. A relative conductivity of 1 represents water of the River Amer, which has the lower EC of the two feeding rivers. An increase in the relative conductivity thus represents an increased proportion of water of the

River Nieuwe Merwede. The relative EC pattern within the network indicates that the River Amer feeds the channels in the south of the study area (relative EC below 1.1) during all field campaigns. The small variations in the relative electrical conductivity, in this part of this area (i.e. in T4 and T6) may be attributed to volumes of older water from the River Amer, which is characterized by a relatively large temporal variation (coefficient of variation of 0.26 within a few days) in EC (Rijkswaterstaat 2018). In the southeast and North-eastern part of the study area there is almost no

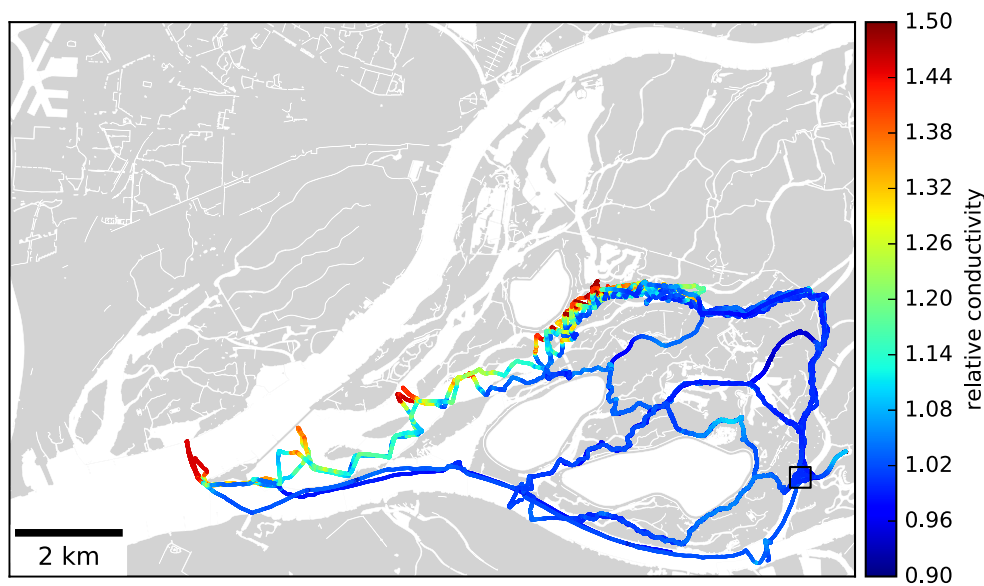


Fig. 8 Electrical conductivity (EC) of the channel water during all field campaigns, relative to the EC as measured across channel section S1 of the side channel of the River Amer (black box). Relative conductivities over 1 represent a higher proportion of water of the River Nieuwe Merwede

contribution of water originating from the Merwede, in spite of the tide-driven changing flow direction in most of these channels.

In channels in the northwestern part of the study area, relative electrical conductivities between 1.3 and 1.5 are found (in S7 and S5, in the northern part of S6, and in the west of S4). These channels transport water from the River Nieuwe Merwede, since they are located downstream of the new river diversions of the River Nieuwe Merwede, originating from the in 2008 and 2015 depoldered areas (yellow and red in Fig. 1). Strikingly, in spite of the tide-driven changing flow direction, there is almost no mixing of water in the major part of the study area. Mixing is only found in the west of side channel section S4, and in sections S6, S8 and S9, in the middle of the study area. These channel sections form the division between water of the Rivers Nieuwe Merwede and Amer, since most water of the River Nieuwe Merwede is found north of and in the northern part of these channels (relative EC of 1.3–1.5), while a relative EC up to 1.1 is found in the south.

A relatively large variation in the relative conductivity is found in section S4. Relative conductivities over 1.1 are distributed further to the east during flood tide and relatively low river discharges of the River Amer, than during ebb tide or during higher discharges of the river Amer. This variation in the distribution of water with a higher relative conductivity is caused by the outflow of water from the in

2008 and 2015 depoldered areas (yellow and red in Fig. 1). This water, originating from the River Nieuwe Merwede, with a higher relative electrical conductivity is mainly found in the northern part of the side channel, but mixing and an eastwards distribution of this water takes place during flood tide and lower river discharges.

Suspended Sediment Load

Figure 9 shows the incoming suspended sediment load (SSL in a, b), and the difference in suspended sediment load (gradient in SSL in c, d) over the channel sections, as average of all field measurements during flood (a, c,) and ebb tide (b, d). All data of the individual measurement campaigns has been aggregated over the respective ebb and flood phase, since no direct significant effect of the river discharge, or smaller tidal periods on the difference in SSL of the river sections was observed for the field campaigns (see Appendix). Figure 9 shows that most side channels have a higher incoming load during ebb than during flood tide, while the incoming load in the tidal channels is higher during flood tide. Furthermore, the incoming load is the highest in side channels sections S4, S6, S8, and S9, located in the northern part of the study area. These channel sections are located downstream of the newly depoldered wetlands, and receive water of the River Nieuwe Merwede, originating from the in 2008 and 2015 depoldered areas (yellow and red in Fig. 1).

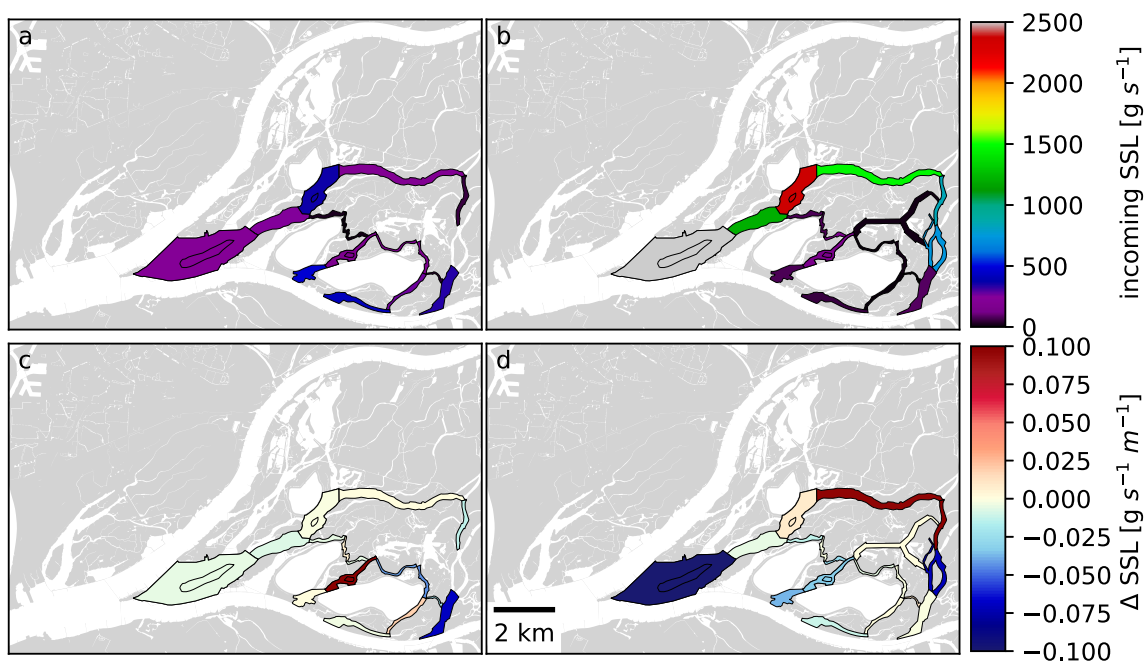


Fig. 9 Incoming suspended sediment Load (SSL; in a, and b), and δ SSL (c, d) of the channel sections for flood (a, c) and ebb tide (b, d)

The gradient in SSL is close to zero in the major part of the study area, especially during flood tide, when the incoming load is small for most channel sections. In contrast, larger differences in SSL are observed during ebb tide in side channel sections S2, S3, S4, S6, and S9.

Although not all channel sections were measured during ebb and during flood tide, the measurements indicate that the major part of the study area functions as a local sink for sediment both during flood and ebb tide. The trapping efficiency of these channel sections is on average 0.18 with a maximum of 0.63. However, it is striking that sections S4 and S6, in the northeast of the study area, function as a sink or experience no change in load during flood tide, but form a source during ebb tide. Furthermore, a positive change in SSL, indicative for erosion, was measured in channel section S4, which is however characterized by a long-term net channel deposition (see Fig. 5). This inconsistency likely arises due the multiple lateral sources of water and sediment in this section, which were not all covered by the measurements in the field campaign. The increase in SSL along these channels is especially large during ebb tide, when lateral sources supply water rich in sediment. This sediment originates both from the newly developed permanent water diversion of the River Nieuwe Merwede (yellow in Fig. 1), and from the tidal channels of the in 2015 depoldered area (red in Fig. 1), which are not represented in the 2007 - 2013 bathymetric changes.

On the other hand, tidal channel section T19, in the center of the study area functions as a source during flood tide and a sink during ebb tide. This channel is located in the middle of the study area, at a relatively large distance from the rivers. The water flow entering these distal channel sections has a low SSL, both during flood and during ebb tide. The low electrical conductivity values (see Fig. 8) with minor variations resulting from volumes of older water, and ionic changes induced by photosynthesis in stagnant water (Talling 2009), indicate that the water originates from the River Amer, which is characterized by a relatively large temporal variation (Rijkswaterstaat 2018). Apparently, no complete flushing occurs here during a tidal cycle, rendering the residence time of the water in this part of the study area to be long, probably in the order of multiple days to weeks.

Discussion

In the present study we used observations at two different time scales to determine the pathways and fate of sediment in a freshwater tidal channel-wetland system, where new wetlands have been developed. These observations

comprised bathymetric maps of the Brabantse Biesbosch Freshwater Tidal Wetland system recorded at a time interval of several years and synoptic field observations of water flow velocity and SSC at a time interval of several weeks. Comparison of the bathymetric maps indicated the channels in the study area function as a sink for sediment, with an average sedimentation rate in the channels of 12.8 mm y^{-1} . Largest changes in bed level, up to 1.38 m y^{-1} , were observed in the newly depoldered wetland (yellow in Fig. 1). These results correspond to those of D'Alpaos et al. (2007) and Vandenbruwaene et al. (2012), who found rapid changes in channel morphology during the first years of newly constructed marshes, until the cross-sectional areas of the channels were in equilibrium with tidal discharge. This tendency towards morphodynamic equilibrium was also identified for a newly depoldered wetland in the Biesbosch, by the analysis of consecutive bathymetric maps by (van der Deijl et al. 2018).

Measurement Survey Changes in SSL measured during our surveys were in general consistent with long-term changes in bed level of the channel sections. This means that the short-term measurements not only help understanding the processes of water and sediment flow through the area, but also allow determining the longer-term development of the major part of the study area. However, a positive change in SSL, indicative for erosion, was measured in channel section S4, in the northeast of the study area, which is characterised by a long-term net channel deposition. This means that although the short-term measurements help understanding the processes of water and sediment flow through the area, they cannot directly be used to predict the longer-term sediment budget of all channel sections in the study area. For this it is necessary that separate synoptic field campaigns are not only combined, but also spatially and temporarily compared to each other. In the case of section S4, the synoptic field measurements indicate that the apparent inconsistency might arise from two likely causes. One is that there are multiple lateral sources of water, and sediment in this section, which were not all covered separately by the measurements in the field campaign. Observed increases in SSL as observed in section S4 were especially large during ebb tide, when lateral sources, originating from the newly developed area, supply water rich in sediment. This high input of sediment from this newly developed area may be explained by the fact that channels have been dug, dikes have been lowered and farmland has been converted to bare intertidal area, which is prone to resuspension by shear stress of wind waves in low water depths (Ford et al. 1999; Braskerud 2001; Pethick 2002;

Mitsch et al. 2014; van der Deijl et al. 2017; Verschelling et al. 2017). The second cause is the temporarily eastward movement of the water and sediment during flood tide, which results in abrupt differences in the suspended sediment concentration over the channel, since almost no mixing takes place with the water, low suspended sediment concentration that comes in from the east. Thus, to develop a full picture of the short-term changes in SSL and to predict the longer-term sediment budget of all channel sections in the study area, additional extensive field campaigns would be needed that focus on the transport and mixing around each lateral source of water. This may reduce the size of the channel sections over which budgets are averaged, and thus would provide a higher spatial detail of the sediment budget in the channel system. Nevertheless, field surveys carried out during short periods of time provide insight in the long-term spatial patterns of sedimentation and erosion, and understanding of how the observed patterns relate to the sources of sediment delivered to, exported from, or stored within the channels and their surrounding lush willow woods, grasslands, and overgrown reed lands. These patterns and system understanding cannot be obtained from high-frequency measurements at only a few monitoring locations. The synoptic measurements of water flow and suspended sediment may be applied to other delta areas elsewhere in the world to identify water and sediment budgets in the delta system, provide insight in the availability of sediment and to select river sections for effective land building diversions. Furthermore, they can be used to assess the effectiveness of newly created river diversions in a short period of time, before new restoration plans are developed.

Within-Wetland Sediment Pathways and Sinks The two rivers are the major source of sediment deposited in the channels of the wetland. Channels with a direct connection to the feeding river supply sediment to the distal parts of the area. Locally, some erosion and internal redistribution of sediment within the wetland channels occur. Upstream supplied sediment is transported in downstream direction through the major side channels of the River Amer and Nieuwe Merwede, but the water flow in most of these channels reverses in direction along with the tides. The sediment load conveyed into the area decreases away from the feeding rivers. Accordingly, the sediment budget for distal channels is relatively low or even negative, both during flood and during ebb tide, compared to the sediment budget of proximal channels.

Most sediment is supplied by the river Nieuwe Merwede, though one inlet in the north. Two major reaches of this channel supply the suspended sediment to the northwest and

north of the study area. Furthermore, tidal currents result in dispersion towards dead-ending channels in the northeast. In spite of the tide-driven changing flow direction in channel section S4, S6, S8 and S9 (Fig. 3), there is almost no mixing of this water with sediment-depleted water of the River Amer (Fig. 8), originating from the East of the study area (S1-S3, Fig. 3). Most water of the River Nieuwe Merwede is flows along the northern bank of these channels, separately from the water of the River Amer along the southern channel bank. Despite the tidal difference in water level, most channels in the north of the study area function as through-flowing side channels of the River Nieuwe Merwede, with a net downstream transport of water. Consequently, these channels receive a new upstream supply of water and sediment each tidal cycle. In contrast, channels in the south are fed by the River Amer, for which the discharge is lower than that of the River Nieuwe Merwede. Hence, the downstream tidally exchanged volume of water is relatively large during conditions of low or average river discharge. As a result, the water body within the channels is not entirely replaced with new river water and sediment during a tidal cycle for these conditions. Instead, the water flow direction may shift in upstream and downstream direction along with the tides, and progressively loses its sediment, resulting in low accumulation rates. Still, new sediment is brought in with the flood phase at the tidal channels, directly connected to the River Amer.

The results from this study indicate that two types of channels can be identified in the study area (see Fig. 10): 1) proximal channels where sediment becomes replenished each tidal cycle; 2) distal channels, which receive water depleted from river sediment. These channel types can be further subdivided in subtype A, B and C. Subtype A comprises dead-ending channels which receive new sediment during the flood phase. Subtype B represent the up- and downstream connected channels, which receive sediment at their downstream connection during the flood phase, and at their upstream connection over the entire tidal cycle. However, when the length and residence time of these channels of subtype B is long enough for depletion of the upstream delivered sediment, the downstream part of this channel becomes subtype C, which has both an upstream and downstream connection to the river, but only a downstream supply of river sediment during the flood phase. The penetration of sediment into the system is influenced by the relative contribution of the tide. Sediment mainly penetrates the upstream part of the system (see Fig. 10a), when tidal flow is relatively low compared to the river discharge. However, sediment mainly penetrates the downstream part of the system, when tidal influence increases (see Fig. 10b).

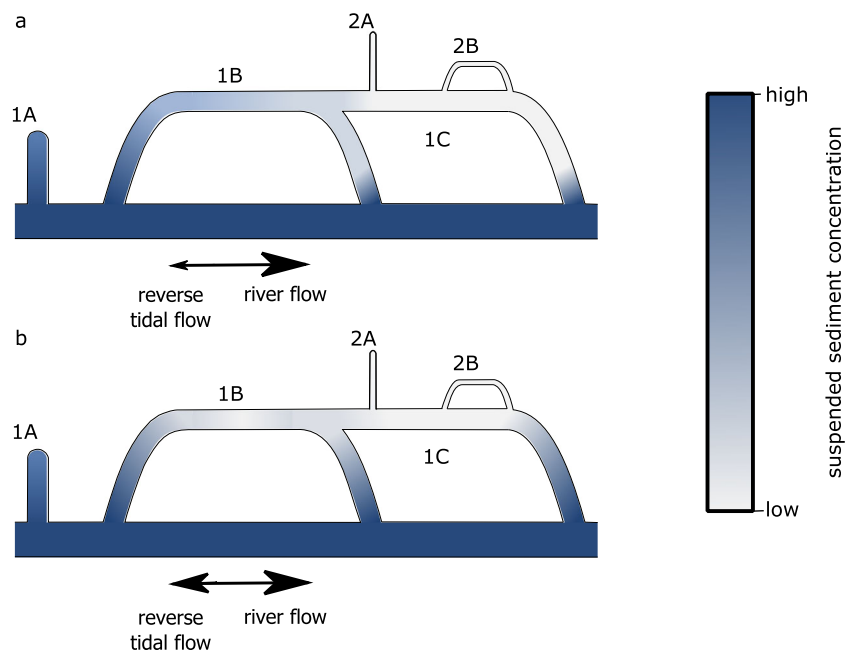


Fig. 10 Generalized channel types and patterns of suspended sediment concentrations in tidal freshwater wetlands dominated by a) river flow (from left to right) and b) both river flow and tidal flow (relative flow is indicated by the arrows). Both figures show two different types of channels as observed in the study area: 1) proximal channels where sediment becomes replenished each tidal cycle; 2) distal channels, which receive water depleted from river sediment. Channel subtype A is comprised of dead-ending channels that only receive new sediment during the flood phase. Subtype B represent the up- and downstream connected channels, which receive sediment throughout the entire tidal

cycle via their upstream connections and via their downstream connection only during the flood phase. When the length and residence time of these channels is long enough for depletion of the upstream delivered sediment, the downstream part of this channel becomes subtype C, which also receives sediment only during the flood phase. In figure a), the tidal influence is relatively small, so sediment mainly penetrates the upstream part of the area. In figure b) the sediment penetrates less far into the river side channel, but during the flood phase, sediment penetrates farther into the downstream reaches of the side channels

In the study area, the sediment budget was the lowest or even negative in channel sections of type 2A and 2B that are far away from the feeding river. Generally, the channels that received the largest volume of river water, and were closer to the rivers had the highest rates of sedimentation. A similar relationship between riverine input of sediment, distance and sedimentation has been shown in other studies. For example, Noe et al. (2016) found greater sedimentation in the upper reaches of freshwater tidal wetlands due to greater availability of fluvial sediment, while sedimentation in the lower reaches of those wetlands was limited, because river sediment load had been exhausted due to settling in the upper reaches. Another example is the study of Lane et al. (2006), who has shown that sites that received the greatest volume of river water and were closer to the new Mississippi diversions had the highest rates of wetland surface elevation increase and vertical accretion. Furthermore, (Mitsch et al. 2014) found higher sedimentation rates closer to the inflow than at the outflow of two flow-through wetlands at the Olentangy River Wetland Research Park (Columbus, Ohio - USA). Studies of Leonard (1997), Reed et al. (1999), van der Deijl et al. (2017), and Verschelling et al. (2017) indicated that also at a smaller scale, the proximity of

the marsh surface to the source of the sediment to be an important factor for deposition. Such relationship between sedimentation and channel position occur at a range of scales.

Enhancing sedimentation by deliberate breaching during floods or redirecting part of the river discharge towards newly developed wetlands is a measure that is often used to prevent drowning (e.g. Giosan et al. 2014; Temmerman and Kirwan 2015). This observational study suggests that the design of new constructed wetlands by river diversions should consider the types of channels in a delta system that we have identified in this study. It is also important to consider the contribution of tide relative to river discharge, because this influences the penetration of sediment into a delta system. An efficient channel wetland lay-out would comprise multiple diverging channels. Especially diversions entering dead ending wetlands should be located close to the feeding river (type 1A and 1C), so river water rich in sediment is transported in each tidal cycle. Through flowing diversions with adjoining wetlands should be limited in length, so not all sediment has been progressively lost with distance from the feeding river. New diversions and wetlands along existing distal channels (type 2A and 2B)

will probably be ineffective for land building, because they will only receive a small volume of water, already depleted from sediment.

Conclusion

This study was performed to identify the pathways for water and sediment transport in freshwater tidal wetlands in a case study for the Brabantse Biesbosch, taking advantage of the differences in geographical setting and boundary conditions of the channels and surrounding within this system. The findings of our study show that the Brabantse Biesbosch functions in general as a sink for sediment. Channel bed sedimentation was on average of 12.8 mm y^{-1} over the period 2007 – 2013, with highest rates in the newly depoldered areas. The two rivers are the major source of sediment, and both the sediment load and the sediment budget decrease with distance away from the feeding rivers.

Within the study area, two different types of channels can be identified that function in a different way in the sediment pathway network of the wetland (Fig. 10) 1) proximal side channels of the rivers; 2) distal tidal channels. Sedimentation takes mainly place in the proximal channels and surrounding wetlands (type 1A), which have an upstream supply of sediment that becomes replenished each tidal cycle. Tidal channels in the middle of the study area, at a large distance from the feeding rivers (type 2A and 2B), experience erosion, since they receive only water poor in sediment during the flood phase.

The results of this investigation complement the insight of earlier studies in both freshwater tidal wetlands, and in oligohaline- and salt marshes of multiple delta areas over the world, that the sediment supply and flow paths to the compartment are factors determining the sediment budget of that compartment. The study shows that the distance of the wetland to the source of the sediment is the major controlling factor of the sediment budget. The tidally exchanged volume of water results in a back and forwards transport of water and sediment. consequently the water body within most channels is not entirely replaced with new river water and sediment during a tidal cycle. However, because of the tidal exchange there is a downstream supply of sediment in dead ending channels during flood tide. When the objective of a new constructed wetland would be using natural sedimentation as a measure for compensating sea level rise and soil subsidence, the design should consider the differences between the three generic types of channels feeding the wetland that we identified in our study. An efficient wetland lay-out would comprise multiple channels of type 1, with limited length, so not all sediment has been progressively lost with distance from the feeding river. Dead ending tidal channels should be located relatively close to

feeding river, so water rich in sediment is transported in at their downstream boundary during the flood phase.

Synoptic moving boat measurements are useful for gaining a quick overview of sediment transport and pathways in deltas within a short period of time. This study shows that synoptic measurements of water flow, EC and SSC were in general consistent with long-term changes in bed level of the channel sections. Therefore, these synoptic measurements can be used to predict the magnitude, direction and mixing of water and sediment fluxes, and the longer-term development in wetland systems in a short period of time. These methods used for this study may be applied to other delta areas elsewhere in the world to identify water and sediment budgets in the delta system, provide insight in the availability of sediment and to select river sections for effective land building diversions. Furthermore, the effectiveness of the newly created river diversions can be assessed in a short period of time, before new restoration plans are developed.

Data Availability

The data for this publication are available via 4TU.Centre for Research Data repository at 10.4121/uuid:5196fe7d-f7a0-43d4-bdbe-e96e8bd7e50b (van der Deijl and van der Perk 2018). It contains:

1. polygons of large channel sections (.shp) (Figs. 2, 5, 9)
2. water surface of the study area (.shp) (Figs. 1, 2, 4–9, 11)
3. polygons of channel sections for VADCP data analysis (.shp) (Figs. 6, 7, 11)
4. Difference in channel bed level for the monitoring period (.TIF) (Figs. 4, 5)
5. Depthmean velocities as measured during the synoptic monitoring campaigns (.csv) (Figs. 6, 7, 11)
6. Suspended sediment concentrations, electrical conductivity, and water depth, as measured during the synoptic monitoring campaigns (.csv) (Figs. 6, 8, 11)

Acknowledgements This project is financed by the Dutch Technology Foundation STW (project nr. 12431). We thank Staatsbosbeheer, Rijkswaterstaat, Dr. Hans de Boois, Sepehr Eslami Arab, Lisanne Braat, Tjalling de Haas, Eelco Verschelling, Daan Wesselman, René Wijngaard and for the provided data, assistance, logistic support, and knowledge.

Open Access This article is distributed under the terms of the Creative Commons Attribution 4.0 International License (<http://creativecommons.org/licenses/by/4.0/>), which permits unrestricted use, distribution, and reproduction in any medium, provided you give appropriate credit to the original author(s) and the source, provide a link to the Creative Commons license, and indicate if changes were made.

Appendix: Raw Data of All Synoptic Sampling Campaigns

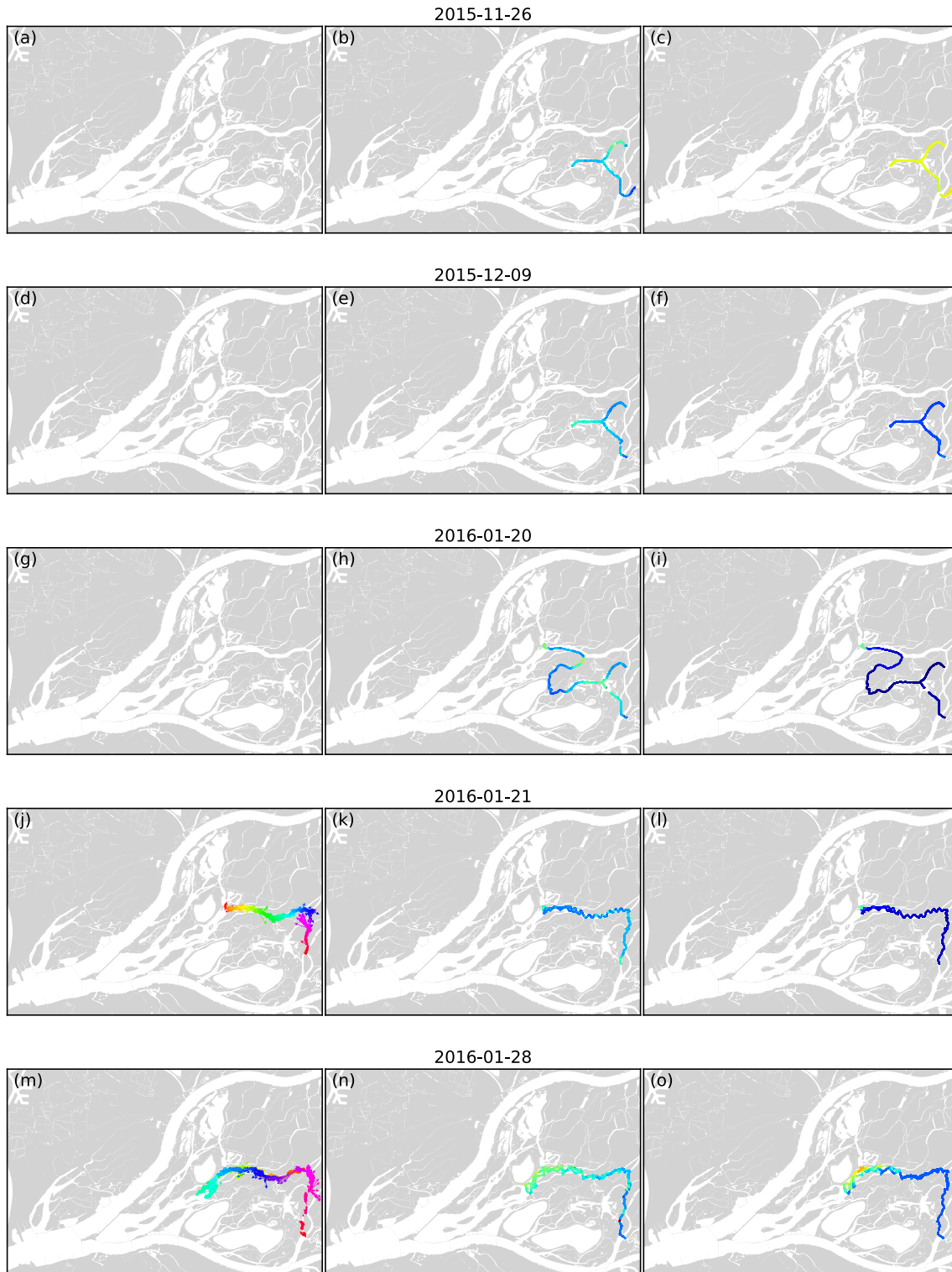


Fig. 11 Flow magnitude and direction during a tidal period (left), suspended sediment concentration (middle), and electrical conductivity (right) of the synoptic sampling campaigns

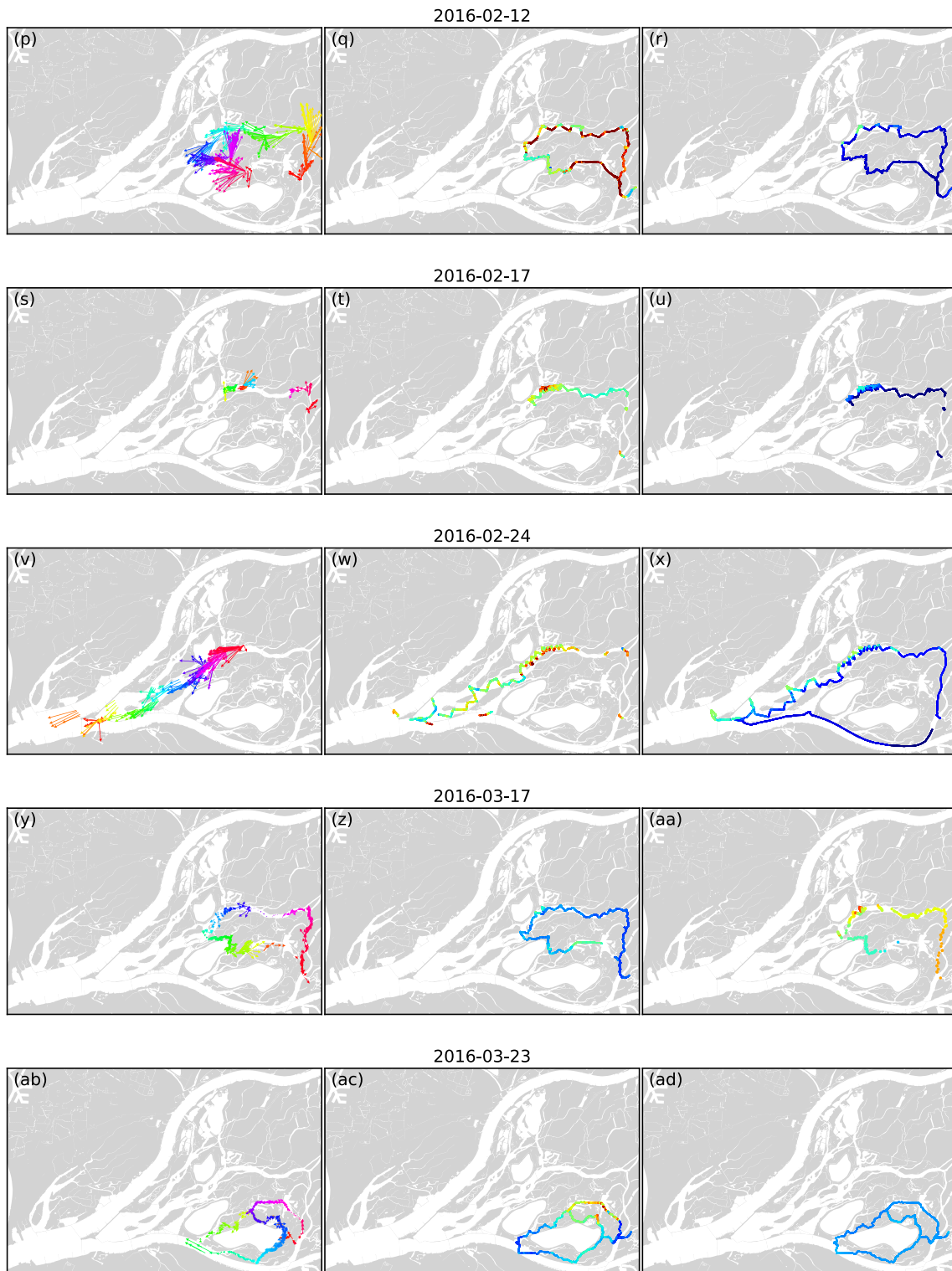


Fig. 12 Flow magnitude and direction during a tidal period (left), suspended sediment concentration (middle), and electrical conductivity (right) of the synoptic sampling campaigns

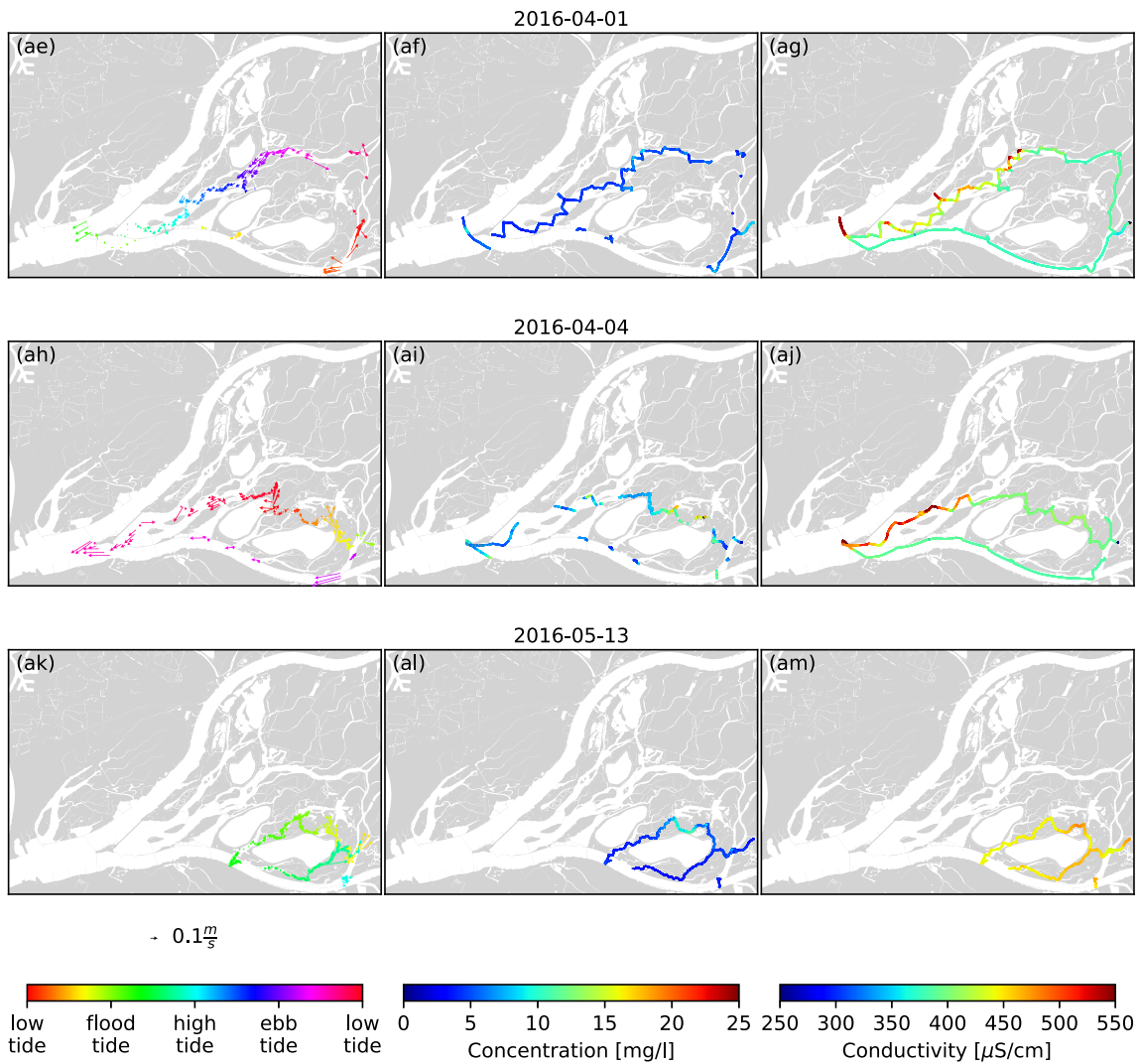


Fig. 13 Flow magnitude and direction during a tidal period (left), suspended sediment concentration (middle), and electrical conductivity (right) of the synoptic sampling campaigns

A.1 SSL of All Synoptic Sampling Campaigns

Table 1 Gradient in SSL [$\text{mg s}^{-1} \text{m}^{-1}$] for different phases in the tidal period

Date	Section	Flood tide					Ebb tide				
		0.2	0.4	0.6	0.8	1.0	1.2	1.4	1.6	1.8	2.0
23-03-2016	S1										-2.4
13-05-2016	S1										
01-04-2016	S1		-69.5								
17-03-2016	S2						0.8				
28-01-2016	S2									9.6	
12-02-2016	S2						-150.3				
17-03-2016	S3						8.8				

Table 1 (continued)

Date	Section	Flood tide					Ebb tide				
		0.2	0.4	0.6	0.8	1.0	1.2	1.4	1.6	1.8	2.0
21-01-2016	S3										
28-01-2016	S3						-13.0			39.2	
12-02-2016	S3							458.8			
23-03-2017	T1								11.8		
13-05-2016	T1		-58.3			3.7					
04-04-2016	T1			-8.9							
23-03-2017	T2									0.3	
13-05-2016	T2					19.0					
23-03-2017	T3									-11.2	
13-05-2016	T3					-2.2					
23-03-2017	T4								-1.3		
13-05-2016	T4			-78.5							
04-04-2016	T4		-6.7								
23-03-2017	T6										-4.2
13-05-2016	T6			-72.3							
04-04-2016	T6		-8.0								
23-03-2017	T7										1.6
17-03-2016	S4					-0.1					
21-01-2016	S4		1.7								
28-01-2016	S4						63.1		107.0		
01-04-2016	S4							13.7			
12-02-2016	S4							110.2			
24-02-2016	S4										189.6
17-03-2016	S6				-1.9						
01-04-2016	S6						90.7				
28-01-2016	S6							51.9	-3.3		
12-02-2016	S6								-52.5		
24-02-2016	S6									62.0	
01-04-2016	S8						-7.8				
04-04-2016	S8										-23.4
24-02-2016	S8									13.1	
01-04-2016	S9					-4.1					
04-04-2016	S9										-132.4
24-02-2016	S9								-401.4		
17-03-2016	T16			-5.5							
04-04-2016	T16										3.6
01-04-2016	T16						-6.2				
12-02-2016	T16								-35.1		
17-03-2016	T17			7.0							
04-04-2016	T17	-0.3									
12-02-2016	T17									-1.7	
23-03-2017	T18								-32.8		
13-05-2016	T18			156.3							
04-04-2016	T18	134.5									

Table 1 (continued)

Date	Section	Flood tide					Ebb tide				
		0.2	0.4	0.6	0.8	1.0	1.2	1.4	1.6	1.8	2.0
17-03-2016	T19			-2.9							
04-04-2016	T19	-6.3									
12-02-2016	T19									-26.8	
23-03-2017	T20									-36.2	
13-05-2016	T20			1.0							

Red colors show positive changes in SSL, indicative for erosion, and blue colors negative changes in SSL, indicative for sedimentation. The colour of the date of the monitoring campaigns represent the Rijkswaterstaat river discharge warning code, for lowered (blue, ± 13 days a year), normal (green, ± 343 days a year), raised (yellow, ± 7 days a year), high (orange, once in 5 to 10 years), or extreme (red, once in 1250 years) river discharge

References

- Braskerud B (2001) The influence of vegetation on sedimentation and resuspension of soil particles in small constructed wetlands. *Journal of Environmental Quality* 30:1447. <https://doi.org/10.2134/jeq2001.3041447x>
- Brouwer R, van Ek R (2004) Integrated ecological, economic and social impact assessment of alternative flood control policies in the Netherlands. *Ecological Economics* 50:1–21. <https://doi.org/10.1016/J.ECOLECON.2004.01.020>
- D'Alpaos A, Lanzoni S, Marani M, Bonometto A, Cecconi G, Rinaldo A (2007) Spontaneous tidal network formation within a constructed salt marsh: observations and morphodynamic modelling. *Geomorphology* 91:186–197. <https://doi.org/10.1016/J.GEOMORPH.2007.04.013>
- de Boois H (1982) Veranderingen in het milieu en de vegetatie in de Biesbosch door afsluiting van het Haringvliet, Ph.D. thesis, Landbouwhogeschool Wageningen, Wageningen <http://library.wur.nl/WebQuery/wurpubs/75774>
- Ford MA, Cahoon DR, Lynch JC (1999) Restoring marsh elevation in a rapidly subsiding salt marsh by thin-layer deposition of dredged material. *Ecological Engineering* 12:189–205
- Giosan L, Syvitski J, Constantinescu S, Day J (2014) Climate change: protect the world's deltas. *Nature* 516:31–33
- Hua Y, Cui B, He W, Cai Y (2016) Identifying potential restoration areas of freshwater wetlands in a river delta. *Ecological Indicators* 71:438–448. <https://doi.org/10.1016/J.ECOLIND.2016.07.036>
- Hudson PF, Middelkoop H, Stouthamer E (2008) Flood management along the Lower Mississippi and Rhine Rivers (The Netherlands) and the continuum of geomorphic adjustment. *Geomorphology* 101:209–236
- Ibáñez C, Day JW, Reyes E (2014) The response of deltas to sea-level rise: Natural mechanisms and management options to adapt to high-end scenarios. *Ecological Engineering* 65:122–130. <https://doi.org/10.1016/j.ecoleng.2013.08.002>
- Lane RR, Day JW, Day JN (2006) Wetland surface elevation, vertical accretion, and subsidence at three Louisiana estuaries receiving diverted Mississippi River water. *Wetlands* 26:779–792. [https://doi.org/10.1672/0277-5212\(2006\)26\[1130:WSEVAA\]2.0.CO;2](https://doi.org/10.1672/0277-5212(2006)26[1130:WSEVAA]2.0.CO;2)
- Leonard LA (1997) Controls of sediment transport and deposition in an incised mainland marsh basin, southeastern North Carolina. *Wetlands* 17:263–274
- Mitsch WJ, Nedrich SM, Harter SK, Anderson C, Nahlik AM, Bernal B (2014) Sedimentation in created freshwater riverine wetlands: 15 years of succession and contrast of methods. *Ecological Engineering* 72:25–34. <https://doi.org/10.1016/J.ECOLENG.2014.09.116>
- Noe GB, Hupp CR, Bernhardt CE, Krauss KW (2016) Contemporary deposition and long-term accumulation of sediment and nutrients by tidal freshwater forested wetlands impacted by sea level rise. *Estuaries and Coasts* 39:1006–1019
- Pethick J (2002) Estuarine and tidal wetland restoration in the United Kingdom: Policy versus practice. *Restoration Ecology* 10:431–437. <https://doi.org/10.1046/j.1526-100X.2002.01033.x>
- Reed DJ, Spencer T, Murray AL, French JR, Leonard L (1999) Marsh surface sediment deposition and the role of tidal creeks: Implications for created and managed coastal marshes. *Journal of Coastal Conservation* 5:81–90
- Rijkswaterstaat (2018) Water data <https://www.watergegevens.rws.nl/>
- Rijkswaterstaat Ruimte voor de Rivier (2016) Ruimte voor de Rivier <https://www.ruimtevoordevier.nl/>
- Talling JF (2009) Electrical conductance – a versatile guide in freshwater science. *Freshwater Reviews* 2(1):65–78. <https://doi.org/10.1608/FRJ-2.1.4>
- Temmerman S, Kirwan ML (2015) NATURAL HAZARDS. Building land with a rising sea. *Science* 349:588–589. <https://doi.org/10.1126/science.aac8312>
- Tessler ZD, Vörösmarty CJ, Grossberg M, Gladkova I, Aizenman H, Syvitski JPM, Foufoula-Georgiou E (2015) Profiling risk and sustainability in coastal deltas of the world. *Science* 349:638–643. <https://doi.org/10.1126/science.aab3574>
- van der Deijl EC, van der Perk M, Middelkoop H (2017) Factors controlling sediment trapping in two freshwater tidal wetlands in the Biesbosch area, The Netherlands. *Journal of Soils and Sediments* 17:2620–2636. <https://doi.org/10.1007/s11368-017-1729-x>
- van der Deijl EC, van der Perk M, Middelkoop H (2018) Establishing a sediment budget in the newly created “Kleine Noordwaard” wetland area in the Rhine–Meuse delta. *Earth Surface Dynamics* 6:187–201. <https://doi.org/10.5194/esurf-6-187-2018>
- van der Deijl EC, van der Perk M (2018) dataset for the article “Pathways of water and sediment in the Biesbosch Freshwater Tidal Wetland”. Utrecht University. Dataset. <https://doi.org/10.4121/uuid:bd1c52a1-74d7-481b-a363-46c29f97c67b>

- Vandenbruwaene W, Meire P, Temmerman S (2012) Formation and evolution of a tidal channel network within a constructed tidal marsh. *Geomorphology* 151-152:114–125
- Verschelling E, van der Deijl E, van der Perk M, Sloff K, Middelkoop H (2017) Effects of discharge, wind, and tide on sedimentation in a recently restored tidal freshwater wetland. *Hydrological Processes* 31:2827–2841. <https://doi.org/10.1002/hyp.11217>
- Zonneveld I (1959) *De Brabantse Biesbosch : A study of soil and vegetation of a freshwater tidal delta consisting of three volumes A, B and C*, Ph.D. thesis, Verslagen Landbouwkundig onderzoek N0.65.20. Bodemkundige studies deel 4, Wageningen. <http://library.wur.nl/WebQuery/wurpubs/487770>